Archives of Biochemistry and Biophysics 538 (2013) 103–110

Contents lists available at ScienceDirect

Archives of Biochemistry and Biophysics

journal homepage: www.elsevier.com/locate/yabbi

UDP-galactopyranose mutases from *Leishmania* species that cause visceral and cutaneous leishmaniasis

Isabel O. Fonseca [a,b], Karina Kizjakina [a,b], Pablo Sobrado [a,b,c,*]

[a] Department of Biochemistry, Virginia Tech, Blacksburg, VA 24061, United States
[b] Fralin Life Science Institute, Virginia Tech, Blacksburg, VA 24061, United States
[c] Virginia Tech Center for Drug Discovery, Virginia Tech, Blacksburg, VA 24061, United States

ARTICLE INFO

Article history:
Received 29 June 2013
and in revised form 21 August 2013
Available online 3 September 2013

Keywords:
Flavin-dependent reaction
Galactofuranose
Non-redox reaction
Neglected diseases

ABSTRACT

Leishmaniasis is a vector-borne, neglected tropical disease caused by parasites from the genus *Leishmania*. Galactofuranose (Gal*f*) is found on the cell surface of *Leishmania* parasites and is important for virulence. The flavoenzyme that catalyzes the isomerization of UDP-galactopyranose to UDP-Gal*f*, UDP-galactopyranose mutase (UGM), is a validated drug target in protozoan parasites. UGMs from *L. mexicana* and *L. infantum* were recombinantly expressed, purified, and characterized. The isolated enzymes contained tightly bound flavin cofactor and were active only in the reduced form. NADPH is the preferred redox partner for both enzymes. A k_{cat} value of $6 \pm 0.4\ s^{-1}$ and a K_m value of $252 \pm 42\ \mu M$ were determined for *L. infantum* UGM. For *L. mexicana* UGM, these values were ~4-times lower. Binding of UDP-Gal*p* is enhanced 10–20 fold in the reduced form of the enzymes. Changes in the spectra of the reduced flavin upon interaction with the substrate are consistent with formation of a flavin-iminium ion intermediate.

Introduction

Malaria, Chagas' disease, and leishmaniasis are diseases caused by protozoan parasites transmitted by insect vectors; consequently, endemic areas are primarily determined by the habitat of the specific vector. These habitats are typically concentrated in tropical/subtropical areas and, thus, mainly affect underdeveloped areas of the world in Central America, South America, Africa, and East Asia. However, human migration and international travel by both private citizens and military personnel provide avenues for the expansion of endemic areas to include other regions of the world. Current treatments for many of the diseases caused by protozoan parasites are ineffective and, therefore, new therapeutic agents are needed [1,2].

In *Leishmania* spp., the causative agent of leishmaniasis, the cell surface is known to contribute to the ability of the parasite to recognize and infect human cells and to evade the host immune system [3,4]. There are three major forms of leishmaniasis: cutaneous, mucocutaneous, and visceral. Symptoms range from self-healing sores observed in cutaneous leishmaniasis to infection of the liver, spleen, and lymph nodes in visceral leishmaniasis. If untreated, leishmaniasis can lead to severe scarring, disfigurement, and death. Leishmaniasis is prevalent in more than 80 countries and estimates from the World Health Organization indicate that 20,000–30,000 people die every year from this disease [5].

The cell surface of *Leishmania* parasites contains lipids and proteins that are glycosylated with the sugar galactofuranose (Gal*f*)[1] [6]. Specifically, Gal*f* is found in the cell surface polysaccharides lipophosphoglycans (LPG) and glycoinositolphospholipids (GIP). LPGs are essential for the binding and detachment of the parasite to the midgut of the insect and, therefore, are required for transmission of the parasite to the human host [7]. Deletion of LPG genes in *Leishmania major* suggests that these glycosylated structures are involved in resistance to oxidative stress and the human immune system, while GIPs have been shown to be essential for growth in *Leishmania mexicana* [8]. Therefore, Gal*f*-containing molecules play important roles in host-specific cell recognition, parasite growth, and pathogenesis. Making enzymes in the Gal*f* biosynthetic pathway potential targets for the development of novel anti-parasitic drugs. One important target is the enzyme UDP-galactopyranose mutase (UGM), which catalyzes the conversion of UDP-galactopyranose to form UDP-Gal*f* (Scheme 1) [9,10]. The importance of this enzyme in kinetoplastids has been validated by demonstration that deletion of the UGM gene leads to greatly reduced virulence in *L. major* [11]. Here, we present the characterization of UGM from *L. mexicana* (*Lmx*UGM) and *Leishmania*

* Corresponding author at: Department of Biochemistry, Virginia Tech, Blacksburg, VA 24061, United States. Fax: +1 540 231 9070.
E-mail address: psobrado@vt.edu (P. Sobrado).

[1] *Abbreviations used:* Gal*f*, galactofuranose; LPG, lipophosphoglycans; GIP, glycoinositolphospholipids; TEV, tobacco etch virus; UGMs, UDP-galactopyranose mutases.

0003-9861/$ - see front matter © 2013 Elsevier Inc. All rights reserved.
http://dx.doi.org/10.1016/j.abb.2013.08.014

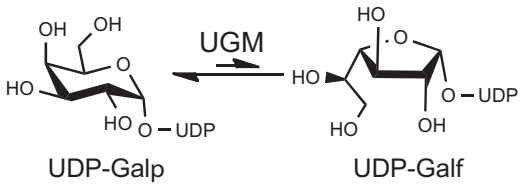

Scheme 1. Reaction catalyzed by UDP-galactopyranose mutase.

infantum (*Lin*UGM), the causative agents of cutaneous and visceral leishmaniasis, respectively.

Materials and methods

Materials

UDP and UDP-galactopyranose were purchased from Sigma. AccuPrime polymerase and *Escherichia coli* TOP-10 chemically competent cells were obtained from Invitrogen (Carlsbad, CA). Restriction endonucleases *Nde*I and *Bam*HI were purchased from New England Biolabs (Ipswich, MA) and *E. coli* BL21 (DE3) chemically competent cells were obtained from Sigma (St. Louis, MO). The plasmid miniprep and PCR purification kits were from Qiagen (Valencia, CA). The genes that code for *L. mexicana* and *L. infantum* UGMs were purchased from GeneScript (Piscataway, NJ). Talon resin was from Clontech (Mountain view, CA). All other buffers and chemicals were purchased from Fisher Scientific (Hampton, NH). Expression vector p11 was obtained from DNASU (http://dnasu.asu.edu/DNASU/Home.jsp).

Cloning

The genes were codon optimized for expression in *E. coli*. The gene for *Lmx*UGM was amplified by PCR using the forward primer 5′-aagccatatgagcgctgataaaaaggtggtgattattg-3′ (*Nde*I site underlined) and the reverse primer 5′-accaggatcctagctcgccgtcggtgccagggtacaac-3′(*Bam*HI site underlined). The synthetic gene coding for *Lin*UGM was amplified using the same forward primer as *Lmx*UGM and the reverse primer 5′-accaggatccttaggaggcggtgctggacagggtgcaac-3′(*Bam*HI site underlined). After running the resulting PCR products on a 0.8% agarose gel, the DNA bands were excised and purified using a Qiagen PCR clean-up kit. The purified samples were digested with the restriction enzymes *Nde*I and *Bam*HI for 2 h at 37 °C and heated for 25 min at 65 °C to stop the reaction. The digested PCR products were then ligated into the expression vector p11, which was previously treated with *Nde*I and *Bam*HI. The target proteins were under control of the T7 promoter and cloned such that the recombinant protein expressed as an N-terminus 8xHis fusion protein. The nucleotide sequences of the final recombinant constructs p11-*Lmxugm* and p11-*Linugm* were confirmed by sequencing.

Protein expression

BL21(DE3) competent cells were transformed with p11-*Lmxugm* or p11-*Linugm* and plated onto LB-agar plates supplemented with 100 μg/mL ampicillin. Colonies (5) were used to inoculate 50 mL LB culture (100 μg/mL ampicillin) and incubated overnight at 37 °C with agitation at 220 rpm overnight. The next morning, six fernbach flasks, each containing 1 L of autoinduction medium (100 μg/mL ampicillin), were inoculated with 10 mL of the overnight culture [12]. The cultures were incubated at 37 °C and agitated at 220 rpm until the optical density at 600 nm (OD_{600}) reached a value of ~3.0. At this point, the temperature was reduced to 18 °C to increase solubility. Twenty hours after the temperature was lowered, the cells were harvested by centrifugation at 5000*g* for 15 min. The resulting cell pellet (~50 g per 6 L of medium) was stored at −80 °C until purification.

Protein purification

*Lin*UGM and *Lmx*UGM were purified following the same procedure. Cell pellets from autoinduction were resuspended in 50 mM sodium phosphate buffer, 300 mM NaCl, 10% glycerol, pH 7.5 containing 25 μg/mL each of lysozyme, DNase, and 0.5 mM PMSF (3 mL of buffer per g of cells). The resuspended cells were stirred for 30 min at 4 °C and disrupted by sonication. The resulting lysate was then centrifuged at 30,000*g* for 50 min at 4 °C to precipitate cell debris and insoluble proteins. The supernatant was collected and loaded onto a Talon column previously equilibrated with buffer A (50 mM sodium phosphate buffer, 300 mM NaCl, 10% glycerol, pH 7.5). The column was washed with 10 column volumes of buffer A and five column volumes of 10% buffer B (50 mM sodium phosphate buffer, 300 mM NaCl, 10% glycerol, 150 mM imidazole, pH 7.5). Bound UGM was eluted using an isocratic gradient with 100% buffer B. Fractions that contained recombinant UGM were identified by the yellow color of the oxidized flavin cofactor. The fractions were pooled and the concentration determined by Bradford assay [13]. To remove the 8xHis tag, tobacco etch virus (TEV) protease was added at a ratio of 1:10 and the sample dialyzed overnight against buffer A. The resulting sample was loaded onto a Talon column and the flow-through containing recombinant UGM was collected. This sample was concentrated and loaded onto a Superdex 75 column equilibrated with 25 mM HEPES, 125 mM NaCl, at pH 7.5. Purified *Leishmania* UGMs were pooled, concentrated, frozen in liquid nitrogen and stored at −80 °C.

UV–visible spectrophotometry

Absorbance data were recorded using an Agilent 8453 UV–visible spectrophotometer. The extinction coefficient of the enzyme-bound FAD was determined by dividing the absorbance value at 450 nm of the bound flavin by the absorbance value at 450 nm of free flavin (obtained by heat denaturation and centrifugation of the recombinant enzyme) and multiplying this value by the extinction coefficient for free FAD (ε_{450} = 11.3 mM^{-1} cm^{-1}).

Mutase activity assay

The activity of the recombinant UGMs was tested by monitoring the formation of UDP-Gal*p* from UDP-Gal*f*. The assay was performed in 100 μL of 25 mM HEPES, 125 mM NaCl, 20 mM sodium dithionite, at pH 7.5, at various concentrations of UDP-Gal*f* (0.02–1.0 mM). The reaction was initiated by addition of 400 nM of *Lin*UGM or 800 nM of *Lmx*UGM. Concentration of target UGM was determined using the flavin extinction coefficient at 450 nm, ε_{450} = 10.5 mM^{-1} cm^{-1}. The reaction was incubated at 37 °C for 2 min and terminated by heat denaturation at 95 °C for 5 min in a PCR thermal cycler. The resulting mixture was filtered (to remove denatured protein) and injected on a Dionex CarboPac™ PA-100 carbohydrate column connected to a Shimadzu Prominence HPLC system. The samples were eluted isocratically with 75 mM KH_2PO_4, pH 4.5, at 0.8 mL/min. Absorbance at 262 nm was monitored to identify fractions containing substrate and product. Under these conditions, UDP-Gal*p* eluted at 25.8 min and UDP-Gal*f* at 32.8 min. The extent of conversion was determined by comparing the areas under the substrate and product peaks. UDP-Gal*f* was synthesized using published protocols [14].

Determination of molecular weight in solution

The molecular weights of *Lmx*UGM and *Lin*UGM were determined using size exclusion chromatography as previously described [15].

Flavin reduction by NAD(P)H

Flavin reduction by NAD(P)H was performed using an Applied Photophysics stopped-flow SX20 spectrophotometer under anaerobic conditions at 15 °C. Oxygen was removed from the stopped-flow system by adding a solution containing 100 mM of glucose and 0.1 mg/mL of glucose oxidase from *Aspergillus niger* (181,300 U/g) in 0.1 M sodium acetate, pH 5.0 overnight. Buffer C (50 mM sodium phosphate pH 7.0) was made under anaerobic conditions with five cycles of vacuum and argon flushing, each for 30 min. NAD(P)H solutions were prepared by dissolving the appropriate amounts in anaerobic buffer C. The concentrations were verified spectroscopically. The enzyme solution was made anaerobic by degassing with six cycles of vacuum for 15 min and flushing with anaerobic argon between cycles. The enzyme (30 μM before mixing) was mixed with various concentrations of NAD(P)H (25–1000 μM after mixing) and the reaction was monitored with a photodiode array spectrophotometer until complete reduction was achieved. Change in absorbance at 452 nm was fit to a single exponential equation and the resulting k_{obs} values were plotted as a function of NAD(P)H concentration. These data were fit with Eq. (1) to obtain the rate constant for reduction (k_{red}) and the K_D value.

$$k_{obs} = (k_{red} * [S])/(K_D + [S]) \quad (1)$$

NADPH oxidation assay

Oxidation of NADPH was monitored at 340 nm for 5 min. Reactions were performed at room temperature with air saturated 50 mM sodium phosphate buffer, pH 7.0, with 125 μM of NADPH, in the presence or absence of 0.5 mM UDP-Gal*p*. The reactions were initiated by addition of 1 or 4 μM of *Lin*UGM or *Lmx*UGM, respectively.

Spectral changes of reduced LmxUGM

The formation of a flavin-iminium ion was determined by monitoring the spectral changes of reduced *Lmx*UGM upon mixing with UDP-Gal*p* or UDP (as control). The assay was performed in the stopped-flow spectrophotometer under anaerobic conditions as described above. Reduced *Lmx*UGM was prepared by addition of 20 mM sodium dithionite. Excess dithionite was removed using a 2 mL desalting column. Reduced *Lmx*UGM at a final concentration of 24 μM was mixed with a final concentration of 0.25 mM UDP-Gal*p* or 0.25 mM UDP. Spectra were collected on a logarithmic time base from 1.3 ms to 2 s using a photodiode array spectrophotometer.

Fluorescence polarization inhibition assay

A fluorescence polarization binding assay was previously developed for bacterial UGMs [16]. This assay was optimized for *Aspergillus fumigatus* UGM [17]. In order to determine whether the *Af*UGM binding assays could be used for *Leishmania* UGMs, the affinity of the UDP-TAMRA chromophore for these enzymes needed to be determined [16,17]. Samples (25 μL) containing *Lin*UGM or *Lmx*UGM (0.001–100 μM) and 30 nM UDP-TAMRA chromophore in 0.05 M sodium phosphate buffer (pH 7.0) were incubated at room temperature for 5–10 min. The samples were transferred to a 96-well black half-area flat-bottom plate (Corning, Corning, NY). Each assay was done in triplicate. The assay was also done with the reduced enzyme, which was obtained by addition of 20 mM sodium dithionite prior to the addition of the chromophore. The anisotropy values were measured on a SpectraMax M5 plate reader (Molecular Devices, Sunnyvale, CA). The K_D values of UDP-TAMRA were obtained by fitting the anisotropy data to Eq. (2), where m_1 and m_2 are the minimum and maximum anisotropy values, respectively, m_3 is the K_D value, and C_t represents the total concentration of the UDP-TAMRA chromophore.

$$y = m_1 + (m_2 - m_1)\frac{(x + C_t + m_3) - \sqrt{(x + C_t + m_3)^2 - 4xC_t}}{2C_t} \quad (2)$$

The binding of UDP or UDP-Gal*p* can be determined by measuring the change in the anisotropy of the UGM–UDP–TAMRA complex as the added ligand competes for the binding site. The assays contained 10 μM *Lin*UGM or 20 μM *Lmx*UGM, 30 nM UDP-TAMRA chromophore, and varying concentrations of UDP or UDP-Gal*p* in 0.05 M sodium phosphate buffer (pH 7.0). The samples were incubated at room temperature for 5–10 min. Negative control was 20 μM *Lmx*UGM or 10 μM *Lin*UGM with 30 nM UDP-TAMRA and background signal was 30 nM UDP-TAMRA in 0.05 M sodium phosphate buffer (pH 7.0). To obtain the reduced forms of the enzymes, 20 mM sodium dithionite was also added to the mixture prior to the addition of ligands. Anisotropy values were measured in triplicate and the K_D values were obtained by fitting the data to Eq. (3), where m_1 and m_2 are the minimum and maximum anisotropy, respectively, m_3 is the slope, and m_4 is the K_D.

$$y = m_1 + \frac{(m_2 - m_1)x^{m_3}}{m_4^{m_3} + x^{m_3}} \quad (3)$$

Results and discussion

Protein expression and purification

Both enzymes were expressed as a fusion to an 8xHis tag. High levels of expression were observed for both proteins; however, significant amount of insoluble protein were present in the pellet after centrifugation of the complete lysate (not shown). The purification procedure involved only two chromatographic steps, an immobilized metal affinity chromatography (IMAC) step and a size exclusion chromatography step. The purification yield was ~0.25 mg of purified protein per gram of cells. Both proteins were more than 95% pure. The flavin incorporation was 40–60%. The spectra of the bound flavin displayed major peaks at 375 and 450 nm, typical of flavin-containing proteins. The extinction coefficient at 450 nm was 10.5 mM^{-1} cm^{-1} for both enzymes (Fig. 1). This value is very similar to the values reported for *Tc*UGM and *Af*UGM, suggesting a similar environment around the flavin cofactor [14,15].

Structural analysis

L. major, *L. infantum*, and *L. mexicana* are 93–96% identical. Between the *Leishmania* enzymes and the *Tc*UGM and *Af*UGM enzymes, the identity is 60% and 49%, respectively. The residues identified as interacting with UDP-Gal*p* in the structure of the *Af*UGM complex are conserved in all eukaryotic UGMs (Fig. 2). The solution molecular weight for both enzymes was calculated to be 58 kDa by size exclusion chromatography (not shown). These values are very close to the predicted molecular weight based on amino acid composition (54.9 kDa). These results indicate that both *Leishmania* enzymes function as monomers in solution. *Tc*UGM and *Lm*UGM have also been shown to function as monomers, while the bacterial UGMs are dimeric and *Af*UGM is

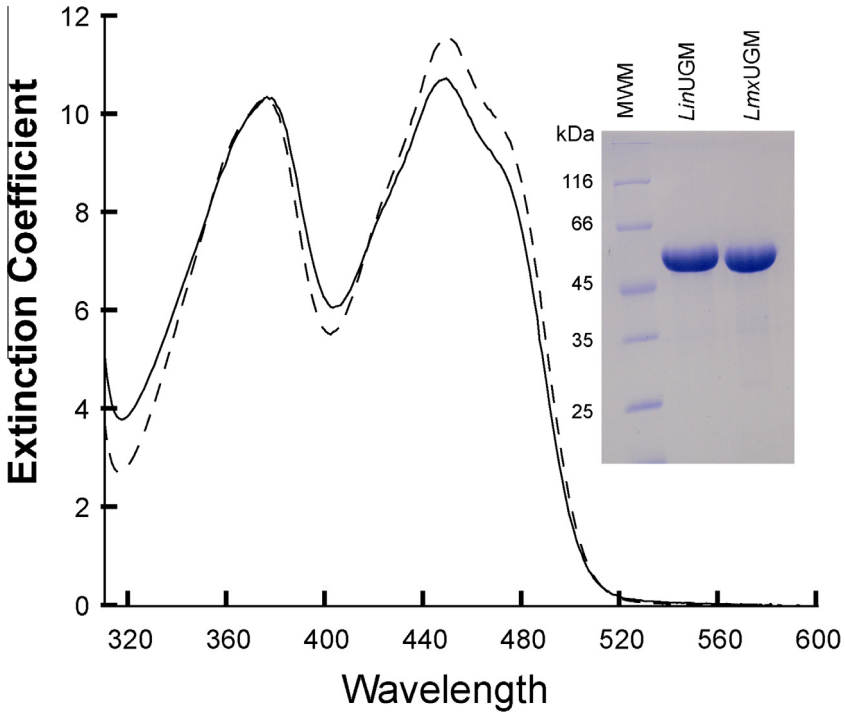

Fig. 1. UV–visible spectra of *Lin*UGM (solid line) and *Lmx*UGM (dashed line). The insert shows a Coomassie blue stained SDS–PAGE of the purified enzymes. (For interpretation of the references to color in this figure legend, the reader is referred to the web version of this article.)

tetrameric [15,18–21]. An explanation for the monomeric composition of the parasitic enzymes was revealed from the structures of *Tc*UGM and *Af*UGM [18,22], which show that an *alpha-helix* at the C-terminus of *Af*UGM, involved in monomer–monomer contact, is missing in the *Tc*UGM structure. The amino acids of this helix are also missing in the *Leishmania* enzymes (C-terminus region, Fig. 2). Similarly, an *alpha-helix* that makes a 4-helix bundle in *Af*UGM contains charged amino acids in the parasitic enzymes, which would lead to charge clashes (aa 113–128 in *Lin*UGM). Thus, the functional form of the *Leishmania* enzymes is most likely monomeric.

Mutase activity

The thermodynamic equilibrium of pyranose to furanose conversion in galactose favors the pyranose form [23,24]. Thus, the activity of the UGMs was determined by measuring the rate of the reverse reaction, UDP-Gal*f* conversion to UDP-Gal*p*, such that product formation is high enough for accurate measurement. Both *Leishmania* UGMs were active only in the reduced form, consistent with all UGMs reported to date [15,25,26]. The reduced form of the enzymes was obtained by addition of 20 mM sodium dithionite. Turnover as a function of UDP-Gal*f* is shown in Fig. 3. Comparison with available data from the other eukaryotic UGMs show that, although there are minor differences between the k_{cat} and K_m values, the catalytic efficiencies (k_{cat}/K_m) are very similar among all eukaryotic enzymes, with the exception of *A. fumigatus* UGM (Table 1) [18,19,27].

Flavin reduction by NADPH

The reaction catalyzed by UGM does not involve a net redox change. However, the reduced form of the flavin cofactor is required for activity [15,28–30]. It has been shown that in the reduced form, the FAD-N5 attacks the UDP-Gal*p* at the C1 position, leading to breaking of the anomeric bond and formation of an FAD-galactose adduct. This adduct is essential for sugar ring contraction [9,14,27,31]. Recently, we showed that *Tc*UGM and *Af*UGM can be reduced by NADPH and to a lesser extent by NADH [14]. For the prokaryotic UGMs, the redox partner has not been identified. We tested whether the *Leishmania* UGMs also use NADPH as their redox partner. The rate of flavin reduction by NADPH can be directly measured by monitoring the bleaching of the absorbance at 452 nm in the stopped-flow spectrophotometer under anaerobic conditions [32–34] (Fig. 4). The k_{red} value for *Lin*UGM was five-times faster than for *Lmx*UGM. Comparison of the available data for other eukaryotic UGMs shows that the k_{red}, and K_D values for NADPH do not significantly vary among the eukaryotic UGMs (Table 2). Flavin reduction was also determined for *Lin*UGM with 3 mM NADH and the k_{obs} value was only 0.04 s^{-1}, suggesting that NADPH is the preferred coenzyme. We recently reported the structure of *Af*UGM in complex with NADP(H) [35]. Site-directed mutagenesis was used to identify residues important in the binding of NADP(H). It was shown that mutation of *Af*UGM R447 and R97 to Ala resulted in a decrease in the rate of reduction by 2000 and 120-fold, respectively [18]. Analysis of the sequence alignment shows that these and other residues predicted to bind NADP(H) are conserved in the *Leishmania* UGMs. Thus, the coenzyme selectivity and reactivity is conserved among eukaryotic UGMs (Fig. 2).

Oxidase activity

The rate of NADPH oxidation by *Leishmania* UGMs was measured under aerobic conditions (Table 3). In this assay, NADPH transfers a hydride to the flavin and the decrease in absorbance at 340 nm accompanied by the formation of $NADP^+$ can be monitored in the spectrophotometer [14]. Since the assay is done in the presence of oxygen, the rate of NADPH oxidation can be monitored as the enzyme reacts with oxygen. The rate of *Lin*UGM at a saturating concentration of NADPH (100 μM) was 0.0200 ± 0.0001 s^{-1}. The rate of oxidation is 300-fold slower than the turnover calculated from the mutase assay. Addition of

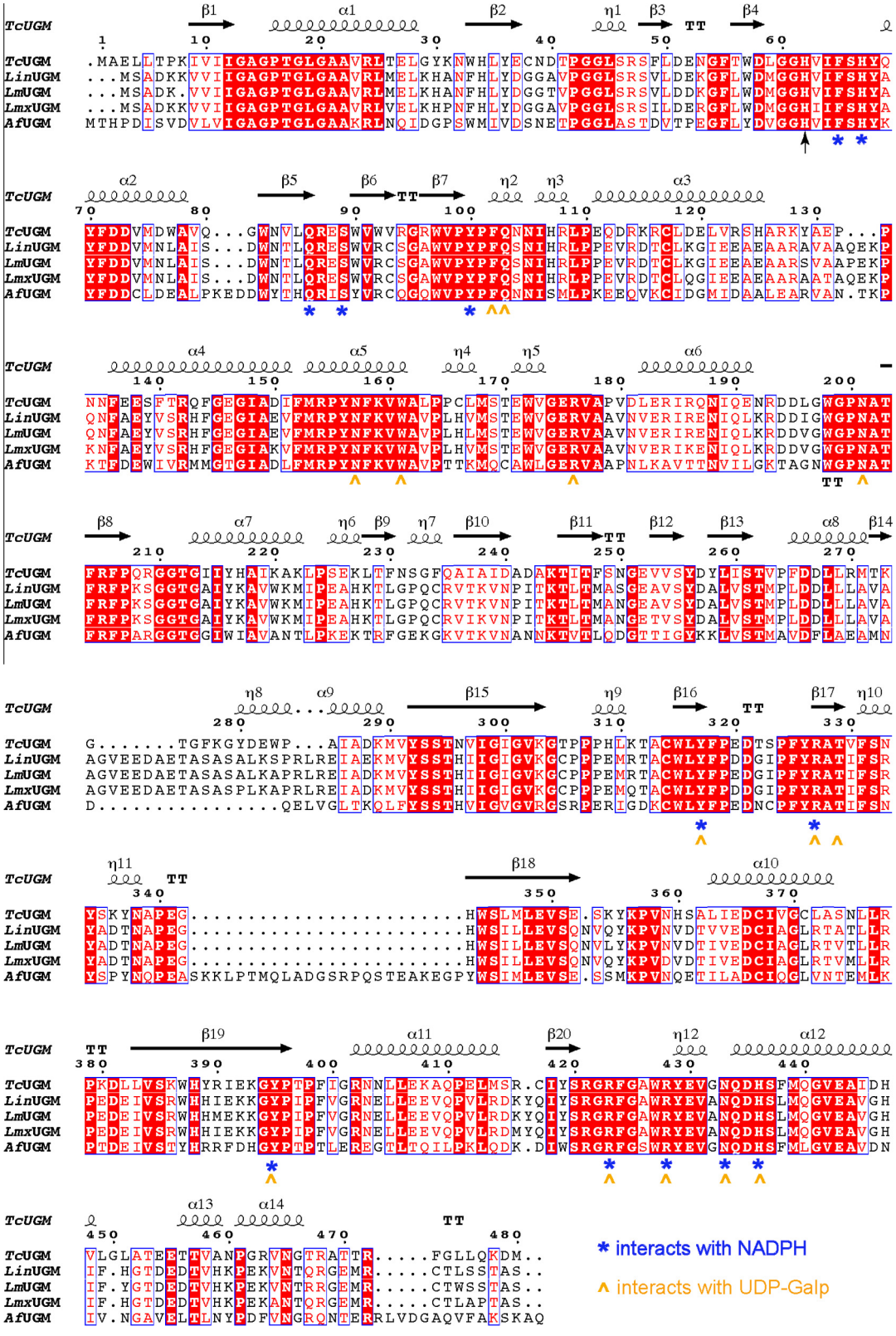

Fig. 2. Amino acid sequence analysis of *T. cruzi* UGM (*Tc*UGM), *L. infantum* UGM (*Lin*UGM), *L. major* UGM (*Lm*UGM), *L. mexicana* UGM (*Lmx*UGM), and *A. fumigatus* UGM (*Af*UGM). Identical amino acids are shown in red boxes and similar amino acids in white boxes. The amino acids involved in NADPH binding are marked with blue asterisks and those that interact with UDP-Gal*p* are marked with orange carets. The conserved His in the histidine loop is marked with an arrow. The structural elements above the sequence are from the *Tc*UGM structure (PDB code 4DSG). Clustal W was used to create the alignment and ESPript 2.2 to create the figure [44]. (For interpretation of the references to color in this figure legend, the reader is referred to the web version of this article.)

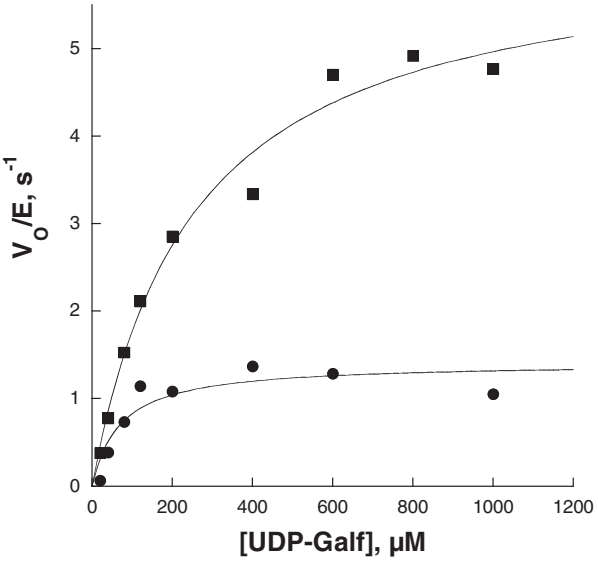

Fig. 3. Steady-state kinetics of *Lin*UGM (squares) and *Lmx*UGM (circles). The initial velocities were calculated by measuring the rate of conversion of UDP-Gal*p* at different UDP-Gal*f* concentrations in the presence of 20 mM dithionite. The data were fit to the Michaelis–Menten equation.

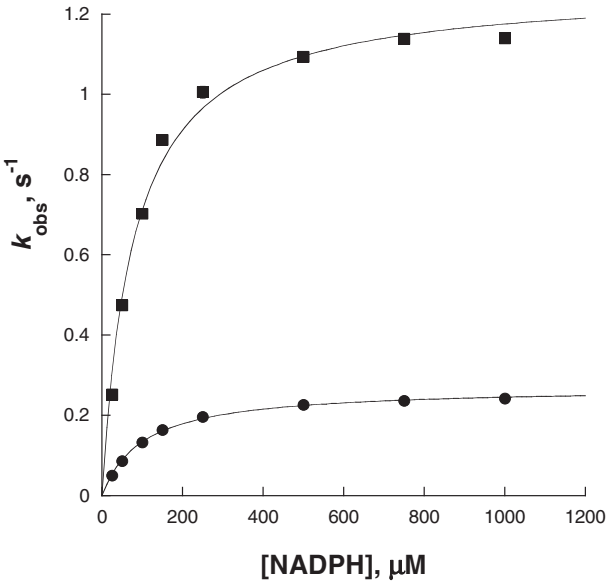

Fig. 4. Rate of flavin reduction by NADPH. The rates of flavin reduction as a function of NADPH concentration under anaerobic conditions were determined in the stopped-flow by following the decrease in absorbance at 452 nm. The data was fit to Eq. (1). The squares are the data for *Lin*UGM and the circles for *Lmx*UGM.

Table 1
Steady-state kinetic parameters of eukaryotic UGMs.

Species	k_{cat} (s^{-1})	K_M (μM)	k_{cat}/K_M, (10^4 M^{-1} s^{-1})	Ref.
L. infantum	6.0 ± 0.4	252 ± 42	2.5 ± 0.3	This work
L. mexicana	1.4 ± 0.2	70 ± 32	2.0 ± 1.0	This work
L. major	5.0 ± 0.2	87 ± 11	5.7 ± 0.6	[19]
T. cruzi	13.0 ± 0.3	140 ± 10	9.3 ± 0.6	[14]
A. fumigatus	72 ± 4	110 ± 15	65 ± 9	[15]
C. elegans	0.61 ± 0.08	8.0 ± 0.8	7.6 ± 1.2	[27]

Conditions: 50 mM sodium phosphate, pH 7.0, at 37 °C using UDP-Gal*f* as substrate in the presence of 20 mM dithionite.

Table 2
Kinetic parameters for the reduction of eukaryotic UGMs by NADPH.

Species	k_{red} (s^{-1})	K_D (μM)	k_{red}/K_D (10^4 M^{-1} s^{-1})	Ref.
L. infantum	1.30 ± 0.03	78 ± 7.8	1.6 ± 0.1	This work
L. mexicana	0.27 ± 0.003	102 ± 4	0.30 ± 0.01	This work
T. cruzi	0.60 ± 0.01	98 ± 3	0.60 ± 0.01	[14]
A. fumigatus	3.0 ± 0.1	25 ± 2	12 ± 1	[35]

Conditions: 50 mM sodium phosphate pH 7.0, under anaerobic conditions at 15 °C.

Table 3
Oxidase activity.

	k_{ox}, (− UDP-Gal*p*l) (s^{-1})	k_{ox}, (+ UDP-Gal*p*l) (s^{-1})
*Lin*UGM	0.020 ± 0.001	0.0120 ± 0.0001
*Lmx*UGM	0.0120 ± 0.0004	0.0060 ± 0.0002

Conditions: 50 mM sodium phosphate, pH 7.0 at 22 °C. The assays contained 125 μM NADPH and UDP-Gal*p* was added at 0.5 mM final concentration.

UDP-Gal*p* decreases the oxidation rate to 0.0120 ± 0.0001 s^{-1}. Since the rate of flavin reduction is 1.3 s^{-1}, it is clear that reduction is not rate-limiting in the oxidase activity of *Lin*UGM. Therefore, the rate-limiting step must be the reaction with molecular oxygen. Similar results are observed with *Lmx*UGM (Table 3). The slow rate of oxidation has significant implications in the mechanism of these enzymes. As mentioned before, the reaction mechanism requires the reduced form of the flavin cofactor for activity. A fast rate of oxidation will result in inactive enzyme and the futile utilization of NADPH. Thus, the *Leishmania* UGMs have evolved a mechanism to stabilize the active reduced form of the flavin, even in the presence of oxygen. A comparison of the rate of oxidation in the presence of UDP-Gal*p* and the k_{cat} values indicate that these enzymes can catalyze >200-mutase reactions before the enzymes become inactivated by oxidation.

Ligand binding

A fluorescence polarization-binding assay was developed for prokaryotic UGMs [16,36]. This assay was based on the fluorescence anisotropy of a UDP-rhodamine or fluorescein chromophore. A modification of the assay was performed where, instead of fluorescein, the chromophore TAMRA was attached to UDP via a five-carbon linker. UDP-TAMRA has five-fold higher affinity for *Af*UGM [17]. We tested the binding affinity of this chromophore for both *Leishmania* UGMs. The results were very similar for both enzymes. Only the results for the *L. infantum* UGM are shown in Fig. 5 for clarity. Addition of higher concentrations of recombinant UGM resulted in an increase in the anisotropy values (Fig. 5A). The data was fit to Eq. (2) to determine the K_D values (Table 4). Since UDP acts as a carrier that directs the chromophore to the active site, titration of ligands that compete for binding to the active site should result in a decrease in the anisotropy value due to the change from the slow tumbling of the chromophore when bound to the protein to the fast tumbling when the chromophore is free in solution. Titration of UDP shows a decrease in the anisotropy, and the change is concentration dependent (Fig. 5B). Similar changes were observed with UDP-Gal*p* (Fig. 5C). The K_D values obtained from fitting the data to Eq. (3), indicate that in the oxidized form, the affinity for UDP is 26–30-fold higher than for UDP-Gal*p* (Table 4). When the enzyme is reduced by addition of excess dithionite, no significant changes in the K_D values for UDP are observed. In contrast, the K_D values for UDP-Gal*p* decrease 5 to 14-fold to values close to UDP (Table 4). Clearly, substrate affinity is enhanced in the reduced forms of the enzymes. The results are consistent with the previously reported values for other

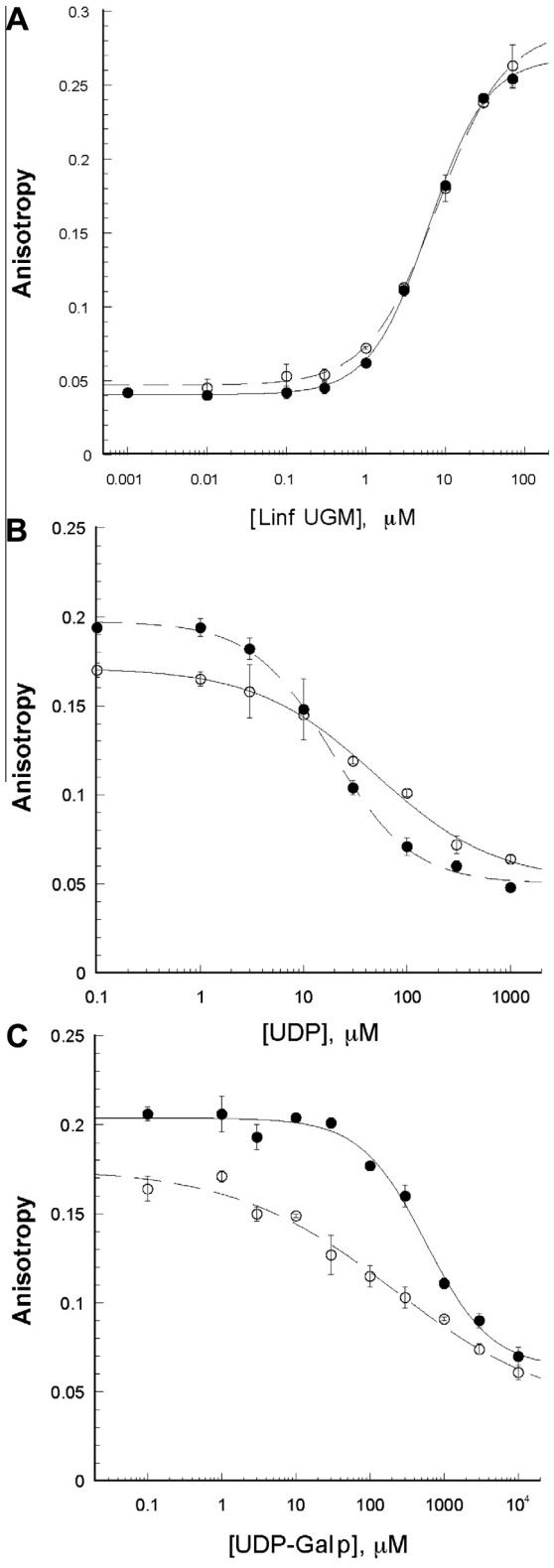

Fig. 5. Fluorescence polarization binding assay. (A) Changes in the anisotropy value of UDP-TAMRA as a function of *Lin*UGM concentration. Changes in the anisotropy of UDP-TAMRA–*Lin*UGM complex as a function of UDP (B) or UDP-Gal*p* (C) concentrations. In all panels, the open circles represent the reduced enzyme and the closed circles represent the oxidized enzyme.

UGMs [10,16,37]. In *Tc*UGM and *Af*UGM, we have shown that reduction of the enzymes is coupled to conformational changes, mainly in a region known as the histidine loop [18,22,38]. The conformational change includes movement of a conserved His residue

Table 4
K_D values for various ligands of *L. infantum* and *L. mexicana* UGMs.

Species	UDP-TAMRA	UDP	UDP-Gal*p*
L. infantum$_{red}$	8 ± 0.3	51 ± 13	110 ± 50
L. infantum$_{ox}$	7 ± 0.6	19 ± 2	580 ± 131
L. mexicana$_{red}$	13 ± 3	97 ± 10	95 ± 6
L. mexicana$_{ox}$	19 ± 7	51 ± 15	1343 ± 212

Conditions: 50 mM sodium phosphate, pH 7.0 at 22 °C. To reduce the enzymes, sodium dithionite (20 mM, final concentration) was added. All the K_D values are in μM.

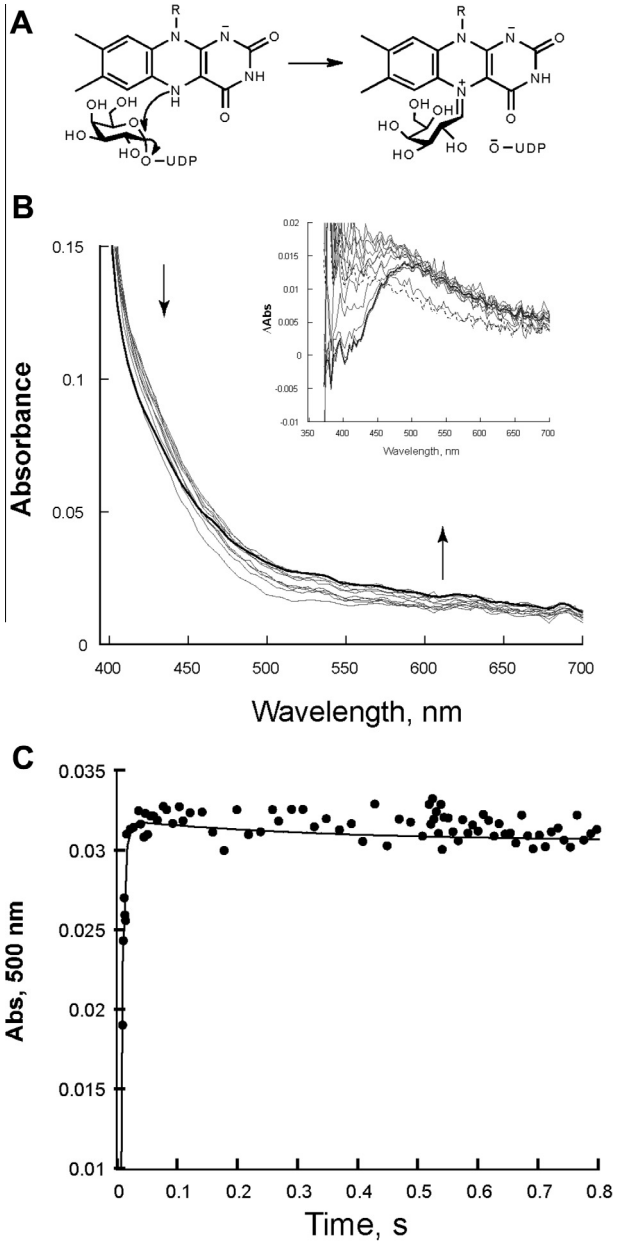

Fig. 6. Detection of flavin-iminium ion. (A) Scheme showing the role of the reduced flavin in UGMs as a nucleophile, which leads to the formation of the flavin-iminium adduct. (B) Changes in the absorbance of reduced flavin in *Lmx*UGM upon mixing with UDP-Gal*p* monitored in the stopped-flow spectrophotometer under anaerobic conditions. The absorbance between 400 and 450 nm decrease, while at values greater than 500 nm increase. The insert shows the absorbance difference. (C) Absorbance change at 500 nm as a function of time. The line is a fit to a double exponential equation.

(His61 in *Lin*UGM) from the substrate binding side of the flavin to the back of the flavin [10,22,38]. This loop is conserved in the *Leishmania* enzymes and it is reasonable to assume that the increase in the affinity in the reduced form may be due to movement of the conserved His such that the Gal*p* portion of the substrate can bind in the active site. The binding of UDP does not change with the redox state of the flavin because the binding site is distant from the cofactor.

Chemical mechanism

In the proposed chemical mechanism of UGMs, a nucleophilic attack by flavin-N5 to the anomeric carbon of UDP-Gal*p* leads to the breaking of the anomeric bond and formation of a flavin-galactose adduct. This is followed by formation of a flavin-iminium ion, sugar ring-opening, and ring-contraction to form galactofuranose. UDP remains bound and attacks the flavin-galactofuranose adduct forming the final product. This flavin-iminium ion has been isolated and characterized in UGMs from *Klebsiella pneumoniae*, *Caenorhabditis elegans*, and *Trypanosoma cruzi* [14,16,20,27]. In addition, structures of several UGMs in complex with UDP-Gal*p*, show that the Gal*p*-C1 and flavin-N5 are aligned and at the favorable distance for nucleophilic attack [20,22,25]. We performed stopped flow experiments with reduced *Lmx*UGM and monitored the reaction after mixing with UDP-Gal*p*. The spectra of the reduced flavin showed the decrease in absorbance between ~400 and ~450 nm, while increase at wavelengths >450 nm (Fig. 6). As a control, the reduced *Lmx*UGM was mixed with UDP, which binds in the active site but cannot react with the flavin, and no changes in the spectrum were observed (not shown). Similar changes in the flavin spectra have been associated with he formation of a flavin derived iminium ion in other UGMs and flavin model systems [9,14,39]. The maximum change in absorbance was observed at 500 nm. A fast rate of $200 \pm 26\ s^{-1}$ and a slow rate of $1.6 \pm 0.4\ s^{-1}$ rate were obtained when the absorbance changes at 500 nm were fitted to a double exponential equation (Fig. 6). We propose that the fast rate corresponds to the formation of the flavin-iminium ion. The slow rate might represent the rate-determining step as it closely matches the value determined for k_{cat}. We propose that the rate-determining step is the ring contraction step to form galactofuranose. This step has been proposed to be the slow step in *T. cruzi* UGM [14]. The results are consistent with the formation of flavin-sugar intermediate and the function of the reduced flavin as a nucleophile in *Leishmania* UGM.

Conclusions

Galactofuranose-containing molecules have been shown to play an important role in the virulence of various *Leishmania* spp. The only known biological source of Gal*f* is via the formation of the UDP-Gal*f* precursor by UGMs [6,10,40]. Deletion of the UGM genes in bacteria, fungi, and *Leishmania* species has shown that the activity of this enzyme is essential or plays an important role in virulence [11,41,42]. In nematodes, the function of UGM has also been proposed to be important in virulence [27,43]. Characterization of the *L. infantum* UGM, the first UGM from a species that causes visceral leishmaniasis, and *L. mexicana* UGM, the second from a species that causes cutaneous leishmaniasis, indicates that these enzymes use NADPH to reduce the flavin. The function of the reduced flavin cofactor as a nucleophile forming a covalent adduct with galactose has been demonstrated in the *Leishmania* enzymes. The availability of active recombinant forms of these enzymes will aid in their structure determination, mechanism-based inhibitor design, and high throughput screening of potential drugs that can be used to treat *Leishmania*-related neglected diseases.

Acknowledgment

This work was supported by NIH Grant R01 GM094469 (P. Sobrado, PI).

References

[1] K. Stuart, R. Brun, S. Croft, A. Fairlamb, R.E. Gurtler, J. McKerrow, S. Reed, R. Tarleton, J. Clin. Invest. 118 (2008) 1301–1310.
[2] R.M. May, Trends Ecol. Evol. 22 (2007) 497–503.
[3] M.J. McConville, S.W. Homans, J.E. Thomas-Oates, A. Dell, A. Bacic, J. Biol. Chem. 265 (1990) 7385–7394.
[4] S.J. Turco, P.A. Orlandi Jr., S.W. Homans, M.A. Ferguson, R.A. Dwek, T.W. Rademacher, J. Biol. Chem. 264 (1989) 6711–6715.
[5] W.H.Organization, http://www.who.int/mediacentre/factsheets/fs375/en/index.html (2013).
[6] S.M. Beverley, K.L. Owens, M. Showalter, C.L. Griffith, T.L. Doering, V.C. Jones, M.R. McNeil, Eukaryot. Cell 4 (2005) 1147–1154.
[7] D.C. Turnock, M.A. Ferguson, Eukaryot. Cell 6 (2007) 1450–1463.
[8] M.A. Ferguson, Philos. Trans. R. Soc. Lond. 352 (1997) 1295–1302.
[9] M. Soltero-Higgin, E.E. Carlson, T.D. Gruber, L.L. Kiessling, Nat. Struct. Mol. Biol. 11 (2004) 539–543.
[10] K. Kizjakina, J.J. Tanner, P. Sobrado, Curr. Pharm. Des. 19 (2013) 2561–2573.
[11] B. Kleczka, A.C. Lamerz, G. van Zandbergen, A. Wenzel, R. Gerardy-Schahn, M. Wiese, F.H. Routier, J. Biol. Chem. 282 (2007) 10498–10505.
[12] B.G. Fox, P.G. Blommel, Curr. Protoc. Protein. Sci. 5 (2009) 23.
[13] M.M. Bradford, Anal. Biochem. 72 (1976) 248–254.
[14] M. Oppenheimer, A.L. Valenciano, K. Kizjakina, J. Qi, P. Sobrado, PLoS ONE 7 (2012) e32918.
[15] M. Oppenheimer, M.B. Poulin, T.L. Lowary, R.F. Helm, P. Sobrado, Arch. Biochem. Biophys. 502 (2010) 31–38.
[16] M. Soltero-Higgin, E.E. Carlson, J.H. Phillips, L.L. Kiessling, J. Am. Chem. Soc. 126 (2004) 10532–10533.
[17] J. Qi, M. Oppenheimer, P. Sobrado, Enzyme Res. 2011 (2011) 513905.
[18] R. Dhatwalia, H. Singh, M. Oppenheimer, P. Sobrado, J.J. Tanner, Biochemistry 51 (2012) 4968–4979.
[19] M. Oppenheimer, A.L. Valenciano, P. Sobrado, Biochem. Biophys. Res. Commun. 407 (2011) 552–556.
[20] T.D. Gruber, W.M. Westler, L.L. Kiessling, K.T. Forest, Biochemistry 48 (2009) 9171–9173.
[21] D.A. Sanders, A.G. Staines, S.A. McMahon, M.R. McNeil, C. Whitfield, J.H. Naismith, Nat. Struct. Biol. 8 (2001) 858–863.
[22] R. Dhatwalia, H. Singh, M. Oppenheimer, D.B. Karr, J.C. Nix, P. Sobrado, J.J. Tanner, J. Biol. Chem. 287 (2012) 9041–9051.
[23] J.N. Barlow, M.E. Girvin, J.S. Blanchard, J. Am. Chem. Soc. 121 (1999) 6968–6969.
[24] P.M. Nassau, S.L. Martin, R.E. Brown, A. Weston, D. Monsey, M.R. McNeil, K. Duncan, J. Bacteriol. 178 (1996) 1047–1052.
[25] S.K. Partha, K.E. van Straaten, D.A. Sanders, J. Mol. Biol. 394 (2009) 864–877.
[26] S.W. Fullerton, S. Daff, D.A. Sanders, W.J. Ingledew, C. Whitfield, S.K. Chapman, J.H. Naismith, Biochemistry 42 (2003) 2104–2109.
[27] D.A. Wesener, J.F. May, E.M. Huffman, L.L. Kiessling, Biochemistry 52 (2013) 4391–4398.
[28] Q. Zhang, H. Liu, J. Am. Chem. Soc. 123 (2001) 6756–6766.
[29] Q. Zhang, J. Am. Chem. Soc. 122 (2000) 9065–9070.
[30] J.N. Barlow, Marcinkeviciene, J., Blanchard, J. S., in: Enzymaic Mechanisms (P.A. Frey, and, D.B. Northrop Eds.), IOS Press, Burke, VA., 1999, p. 98–106.
[31] H.G. Sun, M.W. Ruszczycky, W.C. Chang, C.J. Thibodeaux, H.W. Liu, J. Biol. Chem. 287 (2012) 4602–4608.
[32] E. Romero, R. Robinson, P. Sobrado, J. Vis. Exp. 61 (2012) e38032012. doi:10.3791/3803.
[33] V. Massey, Biochem. Soc. Trans. 28 (2000) 283–296.
[34] S. Ghisla, V. Massey, J.M. Lhoste, S.G. Mayhew, Biochemistry 13 (1974) 589–597.
[35] R. Dhatwalia, H. Singh, L.M. Solano, M. Oppenheimer, R.M. Robinson, J.F. Ellerbrock, P. Sobrado, J.J. Tanner, J. Am. Chem. Soc. 134 (2012) 18132–18138.
[36] E.E. Carlson, J.F. May, L.L. Kiessling, Chem. Biol. 13 (2006) 825–837.
[37] Y. Yuan, X. Wen, D.A. Sanders, B.M. Pinto, Biochemistry 44 (2005) 14080–14089.
[38] K.E. van Straaten, F.H. Routier, D.A. Sanders, J. Biol. Chem. 287 (2012) 10780–10790.
[39] R.F. Williams, T.C. Bruice, J. Am. Chem. Soc. 98 (1976) 7752–7768.
[40] A.G. Trejo, G.J. Chittenden, J.G. Buchanan, J. Baddiley, Biochem. J. 117 (1970) 637–639.
[41] P.S. Schmalhorst, S. Krappmann, W. Vervecken, M. Rohde, M. Muller, G.H. Braus, R. Contreras, A. Braun, H. Bakker, F.H. Routier, Eukaryot. Cell 7 (2008) 1268–1277.
[42] F. Pan, M. Jackson, Y. Ma, M. McNeil, J. Bacteriol. 183 (2001) 3991–3998.
[43] J.F. Novelli, K. Chaudhary, J. Canovas, J.S. Benner, C.L. Madinger, P. Kelly, J. Hodgkin, C.K. Carlow, Dev. Biol. 335 (2009) 340–355.
[44] P. Gouet, E. Courcelle, D.I. Stuart, F. Metoz, Bioinformatics 15 (1999) 305–308.